Oxygen-15-Water PET Assessment of Muscular Blood Flow in Peripheral Vascular Disease

Wolfgang Burchert, Sebastian Schellong, Jörg van den Hoff, Geerd-J. Meyer, Klaus Alexander and Heinz Hundeshagen
Department of Nuclear Medicine and Biophysics and Department of Angiology, Medical School Hannover, Hannover, Germany

To assess quantitatively regional nutritive muscular blood flow in patients with peripheral vascular disease (PVD), we evaluated the utility of PET with ^{15}O-water. **Methods:** Eight healthy volunteers and 16 patients with angiographically proven PVD were studied. Regional blood flow of the calf was measured with ^{15}O-water PET during rest, after intra-arterial infusion of prostaglandin E_1 and during ergometry. The studies were quantified using a one tissue compartment model. **Results:** Normalized mean tracer uptake from 15–60 sec correlated closely ($r = 0.98$) with absolute blood flow. Scan times longer than 90 sec were required to determine blood flow reliably. The flow values were overestimated by 2% if arterial blood volume was neglected or if the input function delay was corrected globally for parametric imaging. Mean blood flow of calf muscles at rest did not differ significantly between patients (0.017 ± 0.006 ml/min/ml) and control subjects (0.018 ± 0.010 ml/min/ml). In PVD patients, blood flow increased by 100% after intra-arterial infusion of PGE_1 in the respective leg. In the control subjects, average flow increased by a factor of six during exercise. The increase was more pronounced in the extensor muscles (0.182 ± 0.031 ml/min/ml) than in flexor muscles (0.121 ± 0.045 ml/min/ml). Due to the specific type of ergometry, superficial flexors exhibited higher flow values than the profound ones. **Conclusion:** PET with ^{15}O-water enables reliable determination of regional nutritive skeletal muscle blood flow for research and clinical applications in patients with PVD.

Key Words: peripheral vascular diseases; PET; muscular blood flow
J Nucl Med 1996; 37:93–98

Inadequate muscle blood flow is the basic pathophysiological principle in peripheral vascular disease (PVD), which causes various clinical symptoms in patients. Diagnosis mainly consists of clinical evaluation, ultrasound studies (*1*) and angiography (*2*). To understand the clinical physiology of the disease and the mode of action of different therapeutic approaches, direct assessment of nutritive muscular blood flow is essential.

Until recently, two methods for direct flow measurement have been widely used: venous occlusion plethysmography (VOP) and ^{133}Xe clearance after intramuscular injection (*3*). VOP has three major drawbacks:

1. Only a combination of cutaneous and muscular blood flow is registered.
2. No identification of the nutritive part of the blood flow is possible.
3. No spatial information is provided (*4*).

A disadvantage of the ^{133}Xe method is that the partition coefficient of the skeletal muscle must be known. This parameter is difficult to obtain and may vary significantly in pathologic conditions (*5*). Moreover, no spatial information is provided. Tracers such as ^{201}Tl (*6–10*) and ^{99m}Tc-sestamibi (*11*) have been proposed for the assessment of regional blood flow in skeletal muscles. Although relative distribution of blood flow can be visualized in planar and tomographic techniques, quantification of absolute blood flow is impossible.

PET has the potential to overcome these difficulties. Initial approaches have been published by Depairon (*12,13*) and Clyne (*14*). Due to methodological insufficiencies, however, no absolute quantification was achieved. It is well established that PET can provide absolute blood flow values for brain (*15–18*), heart (*19*) and tumors (*20*). Therefore, it is desirable to introduce PET for the investigation of PVD as well. To characterize the specific demands for this application, the properties of blood flow measurements in the peripheral skeletal muscle with ^{15}O-water PET have to be evaluated.

MATERIALS AND METHODS

Subjects

We studied 8 male healthy volunteers (mean age: 28.4 ± 3.2 yr) and 16 patients (4 women, 12 men; mean age: 59.6 ± 14.8 yr) with angiographically proven PVD. Twelve of the patients suffered from arteriosclerosis obliterans with occlusion of the femoral-popliteal artery (n = 4), in the tibial arteries (n = 4) or with a combined type of occlusion (n = 4). Four patients had thromboangiitis obliterans with distal and acral arterial occlusions.

Protocols

All subjects were imaged in the supine position with the maximum calf diameter centered in the PET camera. Special attention was given to rest the legs without compression by the patient bed. The tracer was administered through an intravenous line placed in the left cubital vein. The common femoral artery was cannulated according to the Seldinger technique (2 French) to obtain arterial blood samples and to administer drugs. Subjects were allowed to relax for 30 min before the rest study was performed. Three healthy volunteers and seven patients were studied at rest only.

Pharmacological Intervention

Nine PVD patients were studied at rest and after 50 min of intra-arterial infusion of 5 μg prostaglandin E1 into the more severely affected leg. The infusion was stopped only after completion of the PET study to maintain steady-state flow conditions. The contralateral leg served as a control in each case.

Pedal Ergometry

Five healthy volunteers were studied at rest and during pedal ergometry (1–3 Watt per foot), which consisted of rhythmical extension and flexion of the feet fixed at a PET-adapted treadmill with stable support for the legs to avoid movement artifacts. A second transmission scan at the end of exercise confirmed the correct position of the calf. The rotation axes of the pedals were at the position of the ankle joint. The feet were flexed with a 3.85-Nm torque, whereas the extension was supported with a 0.57-Nm torque. The angle of the pedal rotation was measured and summed up over 1 min to assess individual power. The flow study was

Received Sept. 1, 1995; revision accepted Apr. 5, 1996.
For correspondence or reprints contact: W. Burchert, MD, Department of Nuclear Medicine and Biophysics, Radiology Center, Medical School Hannover, Konstanty-Gutschow-Str. 8, 30625 Hannover, Germany.

started 5 min after the start of exercise with a continuous workload until the end of the PET study.

Data Acquisition

The flow studies were acquired with a Siemens/CTI ECAT 951/31 PET scanner. Thirty-one slices with a plane separation of 3.4 mm were obtained simultaneously. The axial and transaxial resolution of the reconstructed image (filtered backprojection, Hann filter, cutoff frequency 0.5, 128 × 128 matrix, pixel size 3.1 mm) was about 8 mm FWHM. After intravenous bolus injection of 1.85 GBq ^{15}O-water, a dynamic scan was acquired (12 × 5 sec, 4 × 15 sec, 2 × 30 sec, 2 × 60 sec; Σ = 5 min). The method for synthesis and automatic bolus injection of ^{15}O-water (about 7 sec) is described elsewhere (*21*). All image data were corrected for attenuation (10-min transmission) and radioactive decay. Arterial blood samples were taken manually from the femoral artery at midframe times through a three-way tap valve. In case of timing problems, protocols were established for actual sampling times. The samples were counted in a well counter and corrected for decay.

Blood Flow Quantification

Parametric blood flow images were calculated as described by van den Hoff et al. (*18*) using a PET-adapted linearization of the Kety-Schmidt model (*22*). This method yields blood flow (f), partition coefficient (p = f/k), fractional arterial blood volume (fbv) and correction for input function delay (Δ), cf. Equation 1, in which c_{PET} denotes tissue activity concentration as measured by PET and c_{art} is the arterial activity concentration.

$$C_{PET}(t) = [(1 - fbv) \cdot f + fbv \cdot k] \int_0^t C_{art}(s + \Delta)\, ds - k \int_0^t C_{PET}(s)\, ds + fbv \cdot C_{art}(t). \quad \text{Eq. 1}$$

Input function delay was determined either individually for dynamic region of interest (ROI) data or globally for parametric maps. Before generation of parametric maps, three-dimensional binomial smoothing (5 pixels in the x, y and z directions, respectively) was applied.

Three types of activity images were compared with quantitative blood flow maps: mean activity from 15 to 60 sec (C_{PET}), mean activity normalized to injected dose (I_0) per body weight (BW) (Eq. 2) and mean activity normalized to injected dose per body surface area (BSA) (Eqs. 3 and 4).

$$SUV_{BW} = \frac{\overline{C_{PET}}}{I_0/BW} \quad \text{Eq. 2}$$

$$SUV_{BSA} = \frac{\overline{C_{PET}}}{I_0/BSA} \quad \text{Eq. 3}$$

$$BSA\ (m^2) = 0.007184 * BW\ (kg)^{0.425} * \text{body weight}\ (cm)^{0.725}. \quad \text{Eq. 4}$$

Image Analysis

ROI definition was performed on the average of nine central slices. Outer leg contours and bones were delineated in the transmission image. The three main arteries were defined on an emission image covering the first 60 sec of the study. Muscle ROIs were defined on an image of the entire emission study using the aforementioned structures as guides. Two separate ROIs were defined for the superficial flexor group (soleus muscle, gastrocnemii muscles) and the deep flexor group (tibialis posterior muscle, flexor hallucis longus muscle, flexor digitorum longus muscle) (Fig. 1).

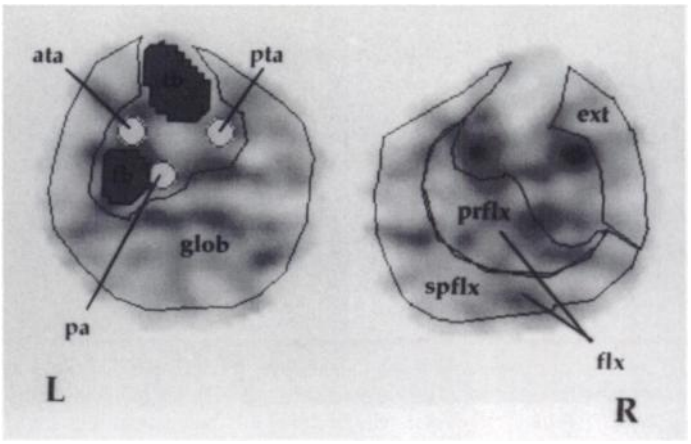

FIGURE 1. ROI definition for regional quantification of muscle blood flow. Parametric blood flow image of a healthy volunteer at rest is shown. Glob = all muscles of the leg; ext = extensor muscles; flx = flexor muscles; spflx = superficial flexor muscles; prflx = profound flexor muscles; tb = tibia; fb = fibula; ata = anterior tibial artery; pta = posterior tibial artery; pa = peroneal artery.

Statistical Analysis

Mean and s.d. were used as descriptive parameters. Linear regression analysis was performed for continuous variables. Unpaired observations were compared by the Mann-Whitney U-test and paired measurements by the Wilcoxon signed-rank-test. Probability values of <0.05 were considered to be significant.

RESULTS

Quantification of Muscular Blood Flow

Typical time-activity curves of a healthy volunteer at rest are shown in Figure 2A. The tissue response curve is rising continuously, reflecting low muscle perfusion. Figure 2B compares tissue-activity curves at rest with the changes induced by marked flow increase during ergometry. During a 300-sec scan time, tissue saturation is achieved only during ergometry.

Quantification of blood flow and partition coefficients may be influenced by several factors. As shown in Figure 3A, scan times greater than 90 sec are required for reliable determination of blood flow, both at rest and during ergometry. However, the partition coefficient cannot be determined under low-flow conditions. Its estimation requires high-flow conditions and scan times of at least 100 sec (Fig. 3B). We obtained a partition coefficient of 0.87 from the high-flow studies.

Another factor is the input function delay, which is due to different locations of blood sampling sites and investigated tissue. Therefore, a variable time shift of the input function has to be included in the fitting procedure for accurate flow estimation. For statistical reasons, the delay has to be determined globally before parametric images can be generated. This may be erroneous in the case of peripheral arterial disease with different time shifts in each leg. The correlation of blood flow derived from parametric images with that of separately fitted ROIs of each leg was very high (r = 0.99; y = 1.02x-0.00015). In parametric images, blood flow was overestimated by about 2%, with 95% of the relative deviations falling within the −2.5 to +5.0% range.

The influence of arterial fractional blood volume was assessed by fitting several datasets with and without inclusion of this parameter. The correlation between both results was very high (r = 0.99; y = 1.02x-0.0002), with a 2% overestimation of flow without correction for fractional blood volume. The

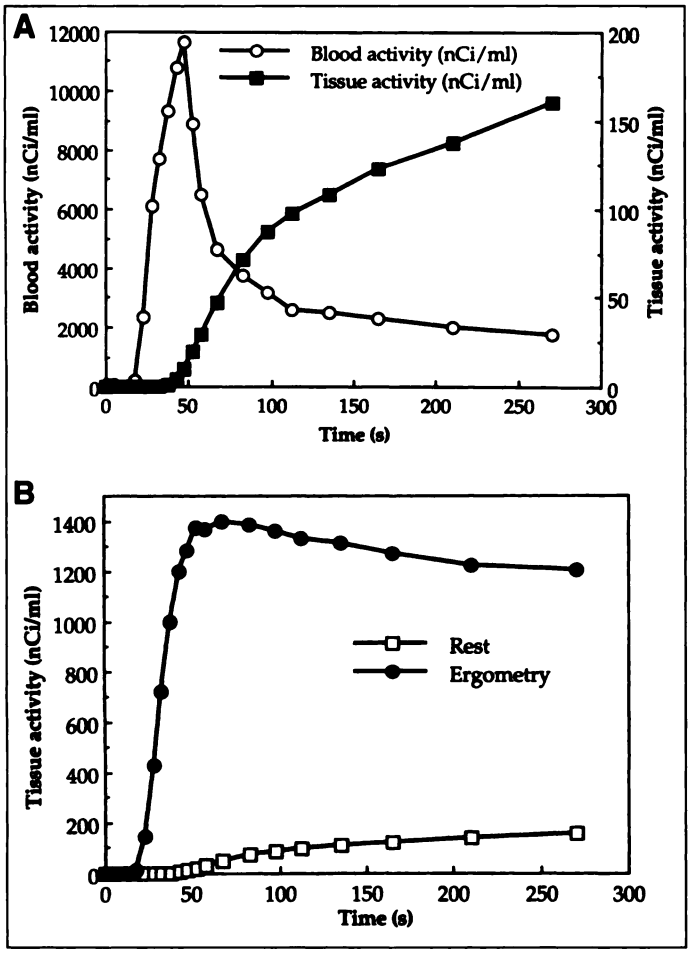

FIGURE 2. Time-activity curves from a healthy volunteer. (A) Arterial input function and tissue response at rest. (B) Tissue time-activity curves during rest and ergometry. The initial curve shapes differ markedly, reflecting different regional blood flow. During scanning, tissue saturation is only achieved during ergometry. Tissue ROIs were placed on the extensor muscle group.

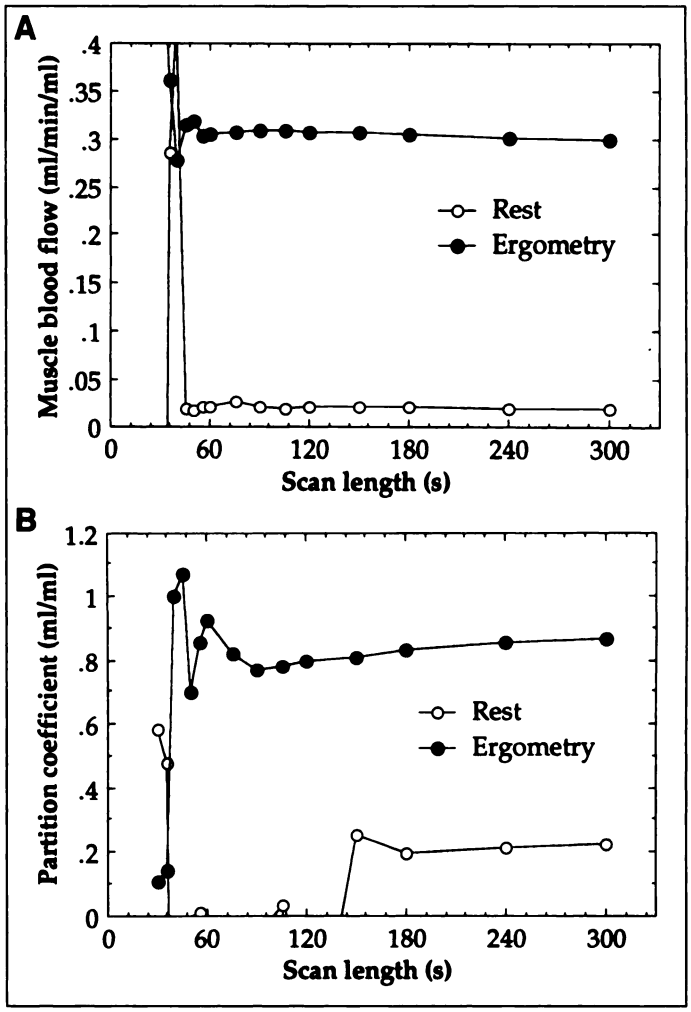

FIGURE 3. Scanning time dependence of blood flow and partition coefficient. Averages of five healthy volunteers are shown. (A) Flow determination is accurate for scan lengths of more than 90 sec for low- (rest) as well as high-flow rates (ergometry). (B) Partition coefficient (pc) is stable for scan times longer than 100 sec during ergometry (pc = 0.87), while no identification of partition coefficient is possible at rest.

comparison of different activity normalization procedures with absolute blood flow yields a close correlation for mean activity ($r = 0.965$; $y = 2455 \times -9$), body weight normalized mean activity ($r = 0.988$; $y = 3.99 \times -0.02$) and activity normalized to body surface area ($r = 0.981$; $y = 10^{-4} \times -5.11 \times 10^{-7}$) (Fig. 4).

CLINICAL STUDIES

Resting Blood Flow

At rest, nutritive muscular blood flow was not significantly different between the control volunteers and patients. In all patients with PVD (n = 32 legs), blood flow was 0.017 ± 0.006 ml/min/ml, whereas blood flow in the control group legs (n = 12 legs) was 0.018 ± 0.009 ml/min/ml.

Pharmacological Intervention

Resting blood flow did not differ significantly between legs in both groups. An average increase in blood flow by a factor of two was observed after infusion of 5 μg prostaglandin E_1 (Fig. 5). Individual variation of the increase was high. Blood flow in noninfused legs showed no significant difference compared to resting conditions, which indicates complete inactivation of PGE_1 before recirculation to the noninfused leg (Table 1).

Pedal Ergometry

Muscle blood flow of the calf increased sixfold during pedal ergometry due to local metabolic demand. Although no differences were found between extensors and flexors at rest, the profound part of the flexors exhibit higher local blood flow than the superficial ones. The extensor muscle group showed higher values during exercise compared to flexor muscles. In all but one subject, the superficial flexors were markedly higher perfused than the profound ones (Table 2, Fig. 6).

DISCUSSION

Methodological Aspects

Measurements with ^{15}O-water have been widely used to assess blood flow quantitatively in the brain and heart (*15–19*). Application of this method to skeletal muscle requires consideration to the peculiarities of this flow territory—notably, very low flow at rest and a large dynamic range of blood flow that can be caused by muscle exercise or pharmacological interventions. Furthermore, during muscle exercise, care has to be taken to avoid motion artifacts that would degrade image resolution.

As for tracer kinetic modeling, the main problems are low count statistics, steady-state flow conditions during imaging sessions, contamination of tissue activity with intravascular tracer, possible nonlinearities of tracer extraction and no tissue activity saturation at rest during longer scan times (> – sec). Despite low tissue activity, sufficient noise reduction can be obtained by three-dimensional smoothing. Additional axial

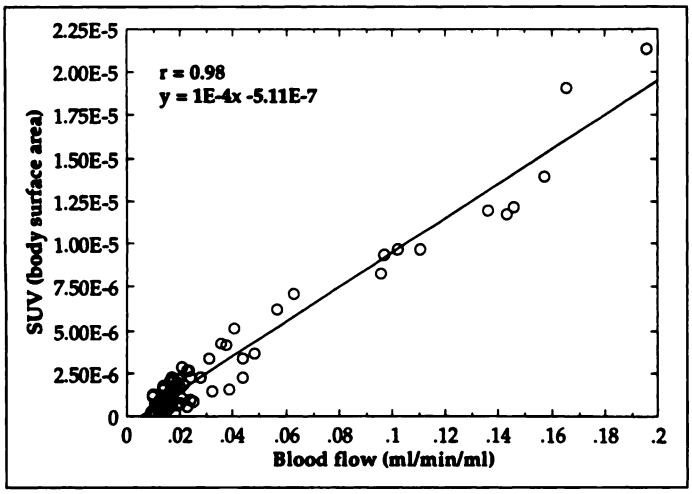

FIGURE 4. Correlation between fitted blood flow values and mean tissue activity from 15 to 60 sec postinjection normalized to body surface area. Accumulated data from all global muscle regions of all subjects.

averaging of up to 3 cm is reasonable because most of the anatomical structures are oriented in the longitudinal direction.

The tracer kinetic model of Kety-Schmidt (*22*) is valid only for steady-state flow conditions. Therefore, any interventional procedure has to be continued for a sufficient time to guarantee steady-state flow conditions.

Because tissue activity concentration is low, any contamination of tissue ROIs with intravascular activity must be avoided. Therefore, the main blood vessels have to be carefully excluded from tissue ROIs. Under these circumstances, fixing the fractional blood volume to zero in the fit caused an average flow overestimation of 2% only. However, for generation of parametric blood flow images, inclusion of the fractional blood volume in the fitting procedure is mandatory. Otherwise very high blood flow values would be calculated in the main blood vessels due to a violation of the tracer kinetic model.

In known applications of flow measurements, ^{15}O-water is considered to be freely diffusible. Deviations from this behavior were only described at very high flow levels, which can be explained as resulting from diffusion limitations, e.g, at the blood-brain barrier for blood flows $\gg$1 ml/min/ml (*23*). In our investigation, such high blood flow values were not observed. The partition coefficient of 0.87 obtained during ergometry supports the assumption that ^{15}O-water is freely diffusible in the skeletal muscle. Under low-flow conditions, the extraction of water is not expected to be limited in any way. Accordingly, the Kety-Schmidt model can be applied to determine muscle blood flow (*18*).

Under low-flow conditions, a monotonous increase of tissue activity was observed. Therefore, no equilibration between blood and tissue was achieved, which prevents determination of the partition coefficient. However, as shown in Figure 3A, the accuracy of the flow determination was not affected by uncertainties in the partition coefficient. The estimated blood flow values were stable for scan times >90 sec in high-flow as well as in low-flow studies.

In PVD patients, impaired blood supply may cause different arrival times of tracer in the tissue. Although a global correction of input function delay for both legs was performed in parametric flow images only, the mean error of this type was limited to 2%. Furthermore, a close correlation over the whole flow

TABLE 1
Global Muscle Blood Flow in Nine Patients with PVD at Rest and After Intra-arterial Administration of Prostaglandin E_1

	PGE+	PGE−	p value
No. of legs	9	9	
Rest	0.018 ± 0.006	0.019 ± 0.003	n.s.
After PGE i.a.	0.036 ± 0.017	0.020 ± 0.010	0.009
p value	0.008	n.s.	

Blood flow values are mean ± s.d. (ml/min/ml). PGE+ = infused legs; PGE− = noninfused legs; After PGE i.a. = after 5 μg prostaglandine E1 intra-arterial over 50 min.

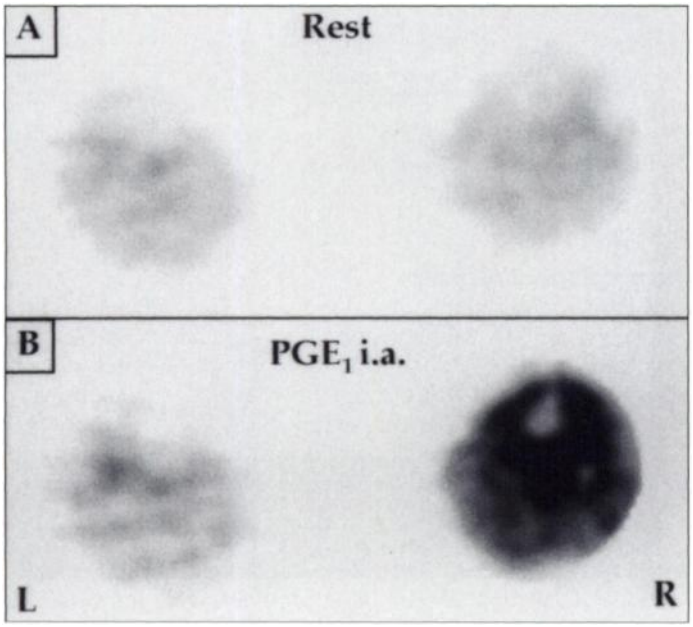

FIGURE 5. Parametric blood flow images of a patient with two-sided peripheral vascular disease. (A) Blood flow at rest. (B) Blood flow at the end of a 50-min intra-arterial infusion of 5 μg prostaglandin E1 (PGE1) into the right femoral artery (A,B) are linearly scaled to a common maximum.

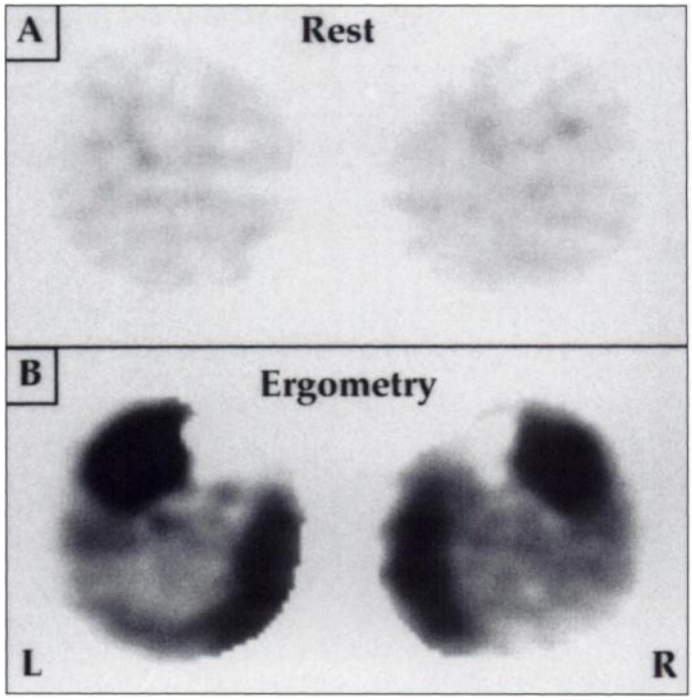

FIGURE 6. Parametric blood flow images of a healthy volunteer. (A) Blood flow at rest. (B) Blood flow during pedal ergometry. Due to the required movement type, blood flow is increased in the anterior tibial muscles and the medial part of the gastrocnemius muscles. A and B are logarithmically scaled to a common maximum because of the large range of flow values.

TABLE 2
Muscle Blood Flow of the Calf in Five Volunteers at Rest and During Pedal Ergometry

	Global	Extensors	Flexors	Extensors vs. flexors (p value)	Superficial flexors	Profound flexors	Superficial vs. profound flexors (p value)
Rest	0.021 ± 0.011	0.021 ± 0.014	0.021 ± 0.011	ns	0.019 ± 0.011	0.026 ± 0.012	0.005
Ergometry	0.135 ± 0.033	0.182 ± 0.031	0.121 ± 0.045	0.022	0.129 ± 0.050	0.097 ± 0.057	ns

Blood flow values are mean ± s.d. (ml/min/ml). ns = not significant.

range was found between globally and regionally corrected data, which justifies the use of parametric images to assess flow.

During pedal ergometry, special care has to be taken to reduce motion artifacts that may deteriorate image resolution substantially. Therefore, specialized ergometry devices which allow maintenance of a stable position for the calf during data acquisition are necessary. Because cyclic thickening of muscles during contraction cannot be avoided, the acquired images average the muscle activity over the corresponding motion. This situation is similar to perfusion imaging of the heart.

Clinical Physiology

Blood flow determinations at rest did not differ between patients and control subjects. The average blood flow of both groups equals 0.018 ± 0.010 ml/min/ml. Both observations are in agreement with results obtained by other authors. Lassen et al. (*3*) reported 0.021 ml/min/ml for control subjects and 0.015 ml/min/ml for patients with no statistically significant difference measured by ^{133}Xe clearance. In an early PET study by Depairon et al. (*13*), a mean of 0.019 ml/min/ml was found in a group of four patients.

Intra-arterial infusion of PGE_1 doubled the resting blood flow in the infused leg, while the contralateral leg showed no changes. This observation might be related to the clinical proven efficacy of the compound in the treatment of Stages III and IV PVD (*24*). Pasch et al. (*25*) reported a 2.5-fold increase in canine hind limb muscles after intra-arterial administration of PGE_1. Other data obtained with venous occlusion plethysmography (*26*) also indicated a flow increase of about 100%. Additionally, our PET study could demonstrate a homogeneous pharmacological effect of PGE_1 on muscular blood flow over all vascular territories of the lower leg.

During ergometry, PET's spatial resolution allowed detection of muscles whose blood flow had changed due to metabolic demand. The average flow increase, which was more pronounced in the extensor than in the flexor muscles, was six times the resting value during exercise, which is in agreement with ^{133}Xe data (*27*). At rest, the profound flexor muscles exhibited significantly higher perfusion than the superficial ones. During ergometry, the superficial muscles had marked higher perfusion than the profound ones except in one subject. This may be due to the fact that the type of workload determines the pattern of muscle involvement. In pedal ergometry, only well-defined motions of the feet are possible, which mainly forces recruitment of the extensors and superficial flexors.

In a more clinical setting, the use of mean activity images during the tracer accumulation phase would allow noninvasive assessment of regional blood flow distribution without arterial blood sampling. In comparison to absolute blood flow, the closest correlations were found in activity images normalized to both body weight and body surface area. Kim et al. (*28*) reported a similar observation for FDG uptake in tumor patients. They preferred normalization to body surface area. Because of this high correlation, PET seems to have potential to provide important and reliable data for regional blood flow distribution with a simplified procedure in clinical use.

Combined regional and quantitative blood flow measurement can only be achieved by PET. Other methods for quantitative measure of blood flow (i.e., ^{133}Xe clearance and VOP) provide insufficient spatial resolution. On the other hand, imaging approaches with planar and tomographic assessment of regional blood flow with ^{201}Tl (*7,8–10,29–34*) and ^{99m}Tc-sestamibi (*11,35*) provide semiquantitative estimates of blood flow only.

CONCLUSION

Dynamic PET with ^{15}O-water is a reliable method to measure regional blood flow in skeletal muscle quantitatively. The observed blood flow changes induced by drug effects and muscle exercise agreed with reported clinical experience and the literature. The possibility to obtain quantitative blood flow values simultaneously with its regional distribution is unique. This feature is advantageous for the characterization of pharmacological and physical therapeutic approaches.

However, the overall radiation burden limits dose response experiments to some well-defined time points that require carefully designed studies. Furthermore, the method cannot detect rapid blood flow changes due to physical and physiological properties of the tracer and limitations of the tracer kinetic model. Therefore, it seems that the main application of ^{15}O-water PET in patients with PVD is the assessment of clinical physiology. However, further experience with this method will also provide clinically useful information.

ACKNOWLEDGMENTS

We thank P. Stellmann, RN, and M. Oberbeck, RN, for assisting with patient care, data acquisition and data processing.

REFERENCES

1. Barnes RW. Noninvasive diagnostic assessment of peripheral vascular disease. *Circulation* 1991;83(suppl I):I-20—27.
2. Murray KK, Hawkins IF. Angiography of the lower extremity in atherosclerotic vascular disease. Current techniques. *Surg Clin North Am* 1992;72:767–789.
3. Lassen NA, Lindbjerg J, Munck O. Measurement of blood flow through skeletal muscle by intramuscular injection of xenon-133. *Lancet* 1964;1:686–689.
4. Sumner DS. Volume plethysmography in vascular disease: an overview. In: Bernstein EF, ed. *Noninvasive diagnostic techniques in vascular disease*, 3rd ed. St. Louis: Mosby; 1985: 97–118.
5. Conn HL. Equilibrium distribution of radioxenon in tissue: xenonhemoglobin association curve. *J Appl Physiol* 1961;16:1065–1070.
6. Strauss HW, Karrison K, Pitt B. Thallium-201: noninvasive determination of the regional distribution of cardiac output. *J Nucl Med* 1977;18:1167–1170.
7. Siegel ME, Siemsen JK. A new noninvasive approach to peripheral vascular disease: thallium-201 leg scans. *Am J Roentgenol* 1978;131:827–830.
8. Oshima M, Akanabe H, Sakuma S, Yano T, Nishikimi N, Shionoya S. Quantification of leg muscle perfusion using thallium-201 single-photon emission computed tomography. *J Nucl Med* 1989;30:458–465.
9. Segall GM, Lennon SE, Stevick CD. Exercise whole-body thallium scintigraphy in the diagnosis and evaluation of occlusive arterial disease in the legs. *J Nucl Med* 1990;31:1443–1449.
10. Segall GM, Lang EV, Lennon SE, Stevick CD. Functional imaging of peripheral vascular disease: a comparison between exercise whole-body thallium perfusion imaging and contrast arteriography. *J Nucl Med* 1992;33:1797–1800.
11. Sayman HB, Urgancioglu I. Muscle perfusion with technetium-MIBI in lower extremity peripheral arterial diseases. *J Nucl Med* 1991;32:1700–1703.

12. Depairon M, De Landsheere C, Merlo P, et al. Effect of exercise on the leg distribution of $C^{15}O_2$ and $^{15}O_2$ in normals and in patients with peripheral ischemia: a study using positron tomography. *Int Angiol* 1988;7:254–257.
13. Depairon M, Depresseux JC, Petermans J, Zicot M. Assessment of flow and oxygen delivery to lower extremity in arterial insufficiency: a PET-scan study. Comparison with other methods. *Angiology* 1991;42:788–795.
14. Clyne CAC, Jones T, Moss S, Ensell J. The use of radioactive oxygen to study muscle function in peripheral vascular disease. *Surg Gynecol Obstet* 1979;149:225–228.
15. Frackowiak RS, Lenzi GL, Jones T, Heather JD. Quantitative measurement of regional cerebral blood flow and oxygen metabolism in man using ^{15}O and positron emission tomography: theory, procedure and normal values. *J Comput Assist Tomogr* 1980;4: 727–736.
16. Huang SC, Carson RE, Hoffmann EJ, et al. Quantitative measurement of local cerebral blood flow in humans by positron emission tomography and ^{15}O-water. *J Cereb Blood Flow Metab* 1983;3:141–153.
17. Raichle ME, Martin WRW, Herscovitch P, Mintun MA, Markham J. Brain blood flow measured with intravenous $H_2{}^{15}O$. II. Implementation and validation. *J Nucl Med* 1983;24:790–798.
18. van den Hoff J, Burchert W, Müller-Schauenburg W, Meyer GJ, Hundeshagen H. Accurate local blood flow measurements with dynamic PET: fast determination of input function delay and dispersion by multilinear minimization. *J Nucl Med* 1993;34:1770–1777.
19. Bergmann SR, Fox KA, Rand AL, et al. Quantification of regional myocardial blood flow in vivo with $H_2{}^{15}O$. *Circulation* 1984;70:724–733.
20. Strauss LG, Conti PS. The application of PET in clinical oncology. *J Nucl Med* 1991;32:623–648.
21. Matzke KH, Meyer GJ, Hundeshagen H. An advanced system for the administration of ^{15}O-water. *J Lab Compd Radiopharm* 1993;32:459–460.
22. Kety SS, Schmidt CE. The nitrous oxide method for the quantitative determination of cerebral blood flow in man: theory, procedure and normal values. *J Clin Invest* 1948;27:476–483.
23. Berridge MS, Adler LP, Nelson AD, et al. Measurement of human cerebral blood flow with ^{15}O-butanol and positron emission tomography. *J Cereb Blood Flow Metab* 1991;11:707–715.
24. Gruss JD, Vargas-Montano H, Bartels T, et al. Use of prostaglandins in arterial occlusive diseases. *Int Angio* 1984;3:7–17.
25. Pasch AR, Burke A, Ricotta JJ, Wilson G, DeWeese JA. Intra-arterial prostaglandin E1 and canine hind limb blood flow. *Curr Surg* 1983;40:289–291.
26. Rexroth W, Amendt K, Römmele U, Stein U, Wagner E, Hild R. Effects of prostaglandin E1 on hemodynamics and leg metabolism in healthy subjects and patients with stage III and IV arterial occlusive disease. *Vasa* 1985;14:220–224.
27. Lassen NA. Muscle blood flow in normal man and in patients with intermittent claudication evaluated by simultaneous ^{133}Xe and ^{24}Na clearances. *J Clin Invest* 1964;43:1805–1812.
28. Kim CK, Gupta NC, Chandramouli B, Alavi A. Standardized uptake values of FDG: body surface area correction is preferable to body weight correction. *J Nucl Med* 1994;35:164–167.
29. Seder JS, Botvinik EH, Rahimtoola SH, Goldstone J, Price DC. Detecting and localization peripheral arterial disease: assessment of ^{201}Tl scintigraphy. *Am J Roentgenol* 1981;137:373–380.
30. Siegel ME, Stewart CA, Kwong P, Sakimura I. Thallium-201 perfusion study of the ischemic ulcers of the leg: prognostic ability compared with doppler ultrasound. *Radiology* 1982;143:233–235.
31. Burt RW, Mullinix FM, Schauwecker DS, Richmond BD. Leg perfusion evaluated by delayed administration of thallium-201. *Radiology* 1984;151:219–224.
32. Hamanaka D, Odori T, Maeda H, Ishii Y, Hayakawa K, Torizuku K. A quantitative assessment of scintigraphy of the legs using ^{201}Tl. *Eur J Nucl Med* 1984;9:12–16.
33. Creutzig H, Creutzig A, Alexander K, Hundeshagen H. Scintigraphy of the heart and skeletal muscle with ^{201}Tl. *Z Kardiol* 1985;74:1–4.
34. Richter W, Beneke R, Barzen G, et al. Quantitative ^{201}Tl scintigraphy of the lower limbs in peripheral artery disease. *Nuklearmedizin* 1993;32:11–17.
35. Miles KA, Barber RW, Wraight EP, Cooper M, Appleton DS. Leg muscle scintigraphy with ^{99m}Tc-MIBI in the assessment of peripheral vascular (arterial) disease. *Nucl Med Commun* 1992;13:593–603.

(continued from page 7A)

FIRST IMPRESSIONS

Cystadenoma Serosum Simplex

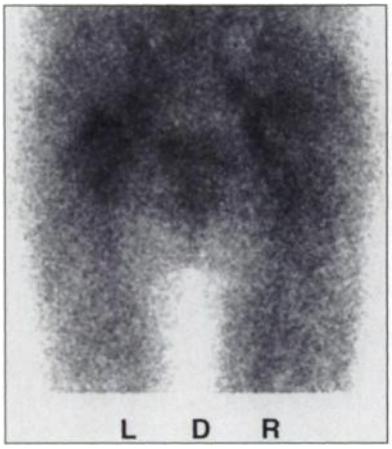

Figure 1.

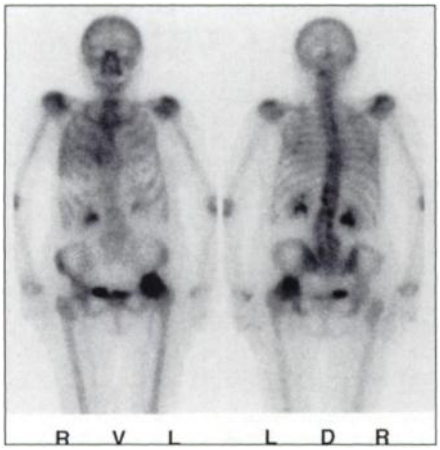

Figure 2.

PURPOSE

We studied an 83-yr-old woman with a history of left hip pain. A three-phase bone scan was performed to rule out inflammation. Anterior views depicted a large, circular photon-deficient area in the pelvis in the flow and early postinjection image (Fig. 1). Two and half hours after injection (Fig. 2), no abnormal abdominal distribution of the tracer was noticed. The left hip showed increased activity due to arthrosis.

Inspection and palpation revealed a persistent large bulge in the lower abdomen. Percussion resulted in ventral sound absorption and tympanic sound at the flanks. These findings did not change with body position. Ultrasonography demonstrated a single-chambered liquid area measuring 15 cm in diameter. Tumor markers (CA-125, CEA, AFP, ß-hCG) were negative. Laparotomy revealed a cystic ovary tumor. Histology: cystadenoma serosum simplex.

TRACER

Technetium-99m-DPD (543 MBq)

ROUTE OF ADMINISTRATION

Intravenous

TIME AFTER INJECTION

5-7 minutes

INSTRUMENTATION

ADAC Genesis large field of view, dual-head, with LEHR collimation

CONTRIBUTORS

U. Schedel, W. Martin and W.H. Knapp, University of Leipzig, Germany